

should not only be able to provide a guide as to the range of validity for the classical continuum theory of solvation relaxation but should also clarify which aspects of solvent molecularity are important in the solvation response and need to be included in microscopic theories of nonequilibrium solvation. From the present work and other simulations<sup>5,9-11</sup> it is apparent that the solute shape and charge distribution will have a large effect on the particular relaxation mechanism that governs the solvent response to an electronic excitation. For a large polyatomic solute where changes in the atomic charges are small and/or shielded from the solvent by bulky solute groups, the classical cavity model should provide an adequate description of the solvent response to the excitation. When the solute is small and/or there are large surface charges generated, the solvation shell structure and dynamics will dominate the relaxation. For this situation, the forces on the solvent molecules will be large and rapidly varying and the relaxation will occur via nondiffusional translation and rotation. In this regime, the dynamics of the solvation shell speeds up rather than slows down the solvent response compared with the bulk response. Also, we expect in this regime that linear response theory will not adequately describe the relaxation because of the highly anharmonic, impulsive nature of the forces exerted on the solvation shell following the excitation. In this context we note the very surprising results of Bader and Chandler in their recent simulations of photoinduced electron transfer in the aqueous ferrous-ferrous system.<sup>38</sup> They found that linear response theory predicted the nonequilibrium response to a surprising degree of accuracy despite the fact that the reorganization energies associated with the perturbation were very large for their model system. Calculations of the corresponding equilibrium correlation functions of the solvation dynamics of formaldehyde in water are being completed by us for comparison with the nonequilibrium simulations reported in the present paper.

(38) Bader, J.; Chandler, D. *Chem. Phys. Lett.* **1989**, *157*, 501.

The present study of the time dependence of the fluorescence shift for formaldehyde in water complements our recent study of hydration effects on the absorption line shape of this molecule.<sup>16</sup> The choice of formaldehyde was dictated in part by the methods we used to parameterize the excited-state potential surface.<sup>15,17</sup> In the context of time-resolved simulations, we regard formaldehyde as representative of a class of small solute molecules that have a sufficiently large change in the dipole moment upon excitation to couple the solvent response to the fluorescence. The probes of choice for experimental time-resolved-fluorescence studies such as the coumarin dyes<sup>39,40</sup> or bis(4-(dimethylamino)phenyl) sulfone (DMAPS)<sup>41</sup> tend to have much larger dipole moment changes upon excitation than does formaldehyde, but they are also considerably larger polyatomics. Since the details of the solute shape and atomic charges control which of several possible solvent relaxation mechanisms is dominant, it is of considerable interest to carry out simulations on corresponding polyatomic dyes for which nonequilibrium solvation measurements are available. Work along these lines is in progress in our laboratory.

**Acknowledgment.** This work has been supported in part by National Institutes of Health Grants GM-30580 (to R.M.L.) and GM-34111 (to K.K.J.) and by the donors of the Petroleum Research Fund, administered by the American Chemical Society. D.B.K. and J.T.B. have been supported in part by Supercomputer Postdoctoral Fellowships from the New Jersey Commission on Science and Technology. D.B.K. is the recipient of a National Institutes of Health NRSA fellowship. We also acknowledge a grant of supercomputer time from the John Von Neumann Center.

Registry No. HCOH, 50-00-0.

(39) Maroncelli, M.; Fleming, G. R. *J. Chem. Phys.* **1987**, *86*, 6221.  
(40) Kahlow, M. A.; Kang, T. J.; Barbara, P. F. *J. Chem. Phys.* **1988**, *88*, 2372.

(41) Su, S. G.; Simon, J. D. *J. Phys. Chem.* **1987**, *91*, 2693.

## Gas-Phase Inorganic Chemistry: Laser Spectroscopy of Calcium and Strontium Monopyrrolate Molecules

A. M. R. P. Bopegedera,<sup>†</sup> W. T. M. L. Fernando, and P. F. Bernath\*<sup>‡</sup>

Department of Chemistry, University of Arizona, Tucson, Arizona 85721 (Received: November 8, 1989; In Final Form: January 15, 1990)

The gas-phase calcium and strontium monopyrrolate molecules were synthesized by the direct reaction between the metal vapor and pyrrole. The electronic and vibrational structures of these molecules were probed by low-resolution laser techniques. The spectra are consistent with a ring-bonding, ionic,  $M^+(C_4H_4N)^-$  structure of pseudo- $C_{5v}$  symmetry. The assignments of the  $\tilde{A}^2E_{1(1/2)}-\tilde{X}^2A_1$ ,  $\tilde{A}^2E_{1(3/2)}-\tilde{X}^2A_1$ , and  $\tilde{B}^2A_1-\tilde{X}^2A_1$  electronic transitions were made by analogy to the isoelectronic metal monocyclopentadienide molecules,  $CaC_5H_5$  and  $SrC_5H_5$ .

### Introduction

Although cyclopentadienyl compounds are very common, the isoelectronic pyrrolyl derivatives are rare.<sup>1</sup> Only a few molecules such as  $(C_5H_5)Fe(C_4H_4N)^2$  and  $(C_4H_4N)Mn(CO)_3$ <sup>3,4</sup> have been characterized. The neutral pyrrole molecule can also serve as a ligand, for example,  $[C_4H_4NH]Cr(CO)_3$ .<sup>5</sup>

Very recently, the replacement of hydrogen atoms by methyl groups was found to increase the stability of pyrrolyl-metal complexes analogous to the effect in cyclopentadienyl-metal complexes.<sup>6</sup> This strategy allowed the preparation of a derivative of 1,1'-diazaferrocene,<sup>7</sup>  $[C_4(CH_3)_4N]_2Fe[C_4(CH_3)_4NH]_2$ .

We report the gas-phase synthesis and laser spectroscopic characterization of  $Ca(C_4H_4N)$  and  $Sr(C_4H_4N)$ . These free radicals are isoelectronic with the  $CaC_5H_5$  and  $SrC_5H_5$  molecules

(1) Cotton, F. A.; Wilkinson, G. *Advanced Inorganic Chemistry*, 5th ed.; Wiley-Interscience: New York, 1977; p 1180.

(2) Joshi, K. K.; Paulson, P. L.; Qazi, A. R.; Stubbs, W. H. *J. Organometal. Chem.* **1964**, *1*, 471-475.

(3) King, R. B.; Efraty, A. *J. Organometal. Chem.* **1969**, *20*, 264-268.

(4) (a) Ji, L.-N.; Kershner, D. L.; Rerek, M. E.; Basolo, F. *J. Organometal. Chem.* **1985**, *296*, 83-94. (b) Kershner, D. L.; Rheingold, A. L.; Basolo, F. *Organometallics* **1967**, *6*, 196-198.

(5) Ófele, K.; Dotzauer, E. *J. Organometal. Chem.* **1971**, *30*, 211.

(6) Kuhn, N.; Horn, E.-M.; Zauder, E.; Bläser, D.; Boese, R. *Angew. Chem., Int. Ed. Engl.* **1988**, *27*, 579-580.

(7) Kuhn, N.; Horn, E.-M.; Boese, R.; Angart, N. *Angew. Chem., Int. Ed. Engl.* **1988**, *27*, 1368-1369.

<sup>†</sup> Current address: NOAA, ERL, R/E/AL2, 325 Broadway, Boulder, CO 80303.

<sup>‡</sup> Alfred P. Sloan Fellow; Camille and Henry Dreyfus Teacher-Scholar.

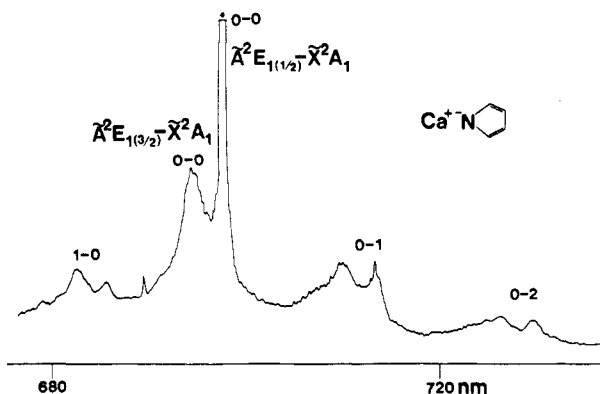


**Figure 1.** The resolved fluorescence spectrum of the  $\tilde{A}^2E_{1(1/2)}-\tilde{X}^2A_1$  transition of calcium monopyrrolate. The laser is tuned to the 0-0 band of the  $\tilde{A}^2E_{1(1/2)}-\tilde{X}^2A_1$  spin component. Collisions connect the  $\tilde{A}^2E_{1(1/2)}$  spin component to the other spin component,  $\tilde{A}^2E_{1(3/2)}$ , which is  $\approx 76\text{ cm}^{-1}$  to the blue of the laser. The wavelength of the laser is marked with an asterisk. The broad features which are  $\approx 300\text{ cm}^{-1}$  to the red and to the blue of the laser are assigned to progressions in the metal-ligand stretching vibration.

previously discovered in our laboratory.<sup>8</sup>

### Experimental Details

The gas-phase reaction between the alkaline-earth metal (Ca, Sr) and pyrrole was used to synthesize the calcium and strontium monopyrrolate molecules. The experimental arrangement was similar to the configuration in our previous work in this area.<sup>8-16</sup> The metal was vaporized in a Broida oven<sup>17</sup> by resistive heating and carried to the reaction region entrained in argon carrier gas. Ground-state metal atoms were found not to react with pyrrole. Ca and Sr atoms were, therefore, excited to the  $^3P_1$  state by using a Coherent 599-01 broad band dye laser tuned to the  $^3P_1-^1S_0$  atomic transition (6573 Å for Ca, 6892 Å for Sr). Pyrrole has a low vapor pressure at room temperature (boiling point = 131 °C). In order to obtain a sufficient flow of pyrrole into the Broida oven, it was necessary to bubble argon through the glass cell containing pyrrole. The total pressure in the oven was about 4 Torr of mainly argon carrier gas. The direct reaction between the excited metal vapor and pyrrole vapor produced the metal monopyrrolates. Analytical grade pyrrole (Alfa Chemical) was used without further purification.

A Coherent 599-01 broad band dye laser operated with DCM or Pyridine 2 laser dyes was used to probe the molecular transitions. Laser excitation spectra were recorded by scanning the wavelength of this laser and recording the total fluorescence from the electronically excited metal monopyrrolate molecules using a photomultiplier-filter combination. Schott RG9 and RG 780 red-pass filters were used to block the scattered laser radiation. The laser resonant with the molecular transition was chopped and the modulated signal was detected with a lock-in amplifier.

Once the frequencies of the two electronic transitions were

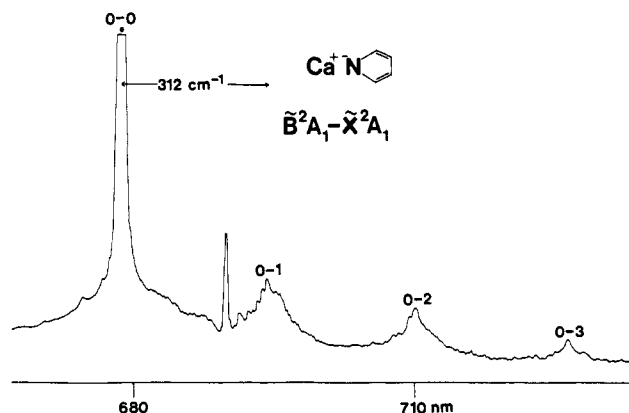


**Figure 2.** The resolved fluorescence spectrum of the  $\tilde{B}^2A_1-\tilde{X}^2A_1$  transition of calcium monopyrrolate. The asterisk marks the position of the laser tuned to the 0-0 band. A progression of vibronic bands in the metal-ligand stretch are clearly seen in the spectrum. The sharp feature just to the left of the 0-1 band is the Sr  $^3P_1-^1S$  atomic line. Sr present as an impurity in the Ca metal and is, presumably, excited by energy transfer from the excited calcium monopyrrolate.

**TABLE I: Band Origins for the Observed Vibronic Transitions of Calcium and Strontium Monopyrrolate Molecules (in  $\text{cm}^{-1}$ )**

band	Ca(C <sub>4</sub> H <sub>4</sub> N)	Sr(C <sub>4</sub> H <sub>4</sub> N)
	$\tilde{A}^2E_{1(1/2)}-\tilde{X}^2A_1$	
2-0	14 830	13 686
1-0	14 584	13 449
0-0	14 333	13 212
0-1	14 021	12 958
0-2	13 714	12 706
0-3		12 455
0-4		12 207
	$\tilde{A}^2E_{1(3/2)}-\tilde{X}^2A_1$	
2-0	14 890	
1-0	14 650	13 770
0-0	14 409	13 512
0-1	14 097	13 257
0-2	13 786	13 004
0-3		12 749
0-4		12 497
	$\tilde{B}^2A_1-\tilde{X}^2A_1$	
2-0		14 069
1-0		13 849
0-0	14 732	13 620
0-1	14 419	13 367
0-2	14 108	13 116
0-3	13 799	12 863
0-4		12 612

obtained from laser excitation spectroscopy, the laser probing the molecular transitions was tuned to the frequency of the electronic transition. Resolved fluorescence spectra were reported by dispersing the laser-induced fluorescence with a 2/3-m monochromator equipped with a GaAs photomultiplier tube and photon-counting electronics.

### Results and Analysis

Some sample low-resolution laser excitation spectra and resolved fluorescence spectra recorded for the Ca(C<sub>4</sub>H<sub>4</sub>N) and Sr(C<sub>4</sub>H<sub>4</sub>N) molecules are given in Figures 1-3. Two electronic transitions,  $\tilde{A}^2E_1-\tilde{X}^2A_1$  and  $\tilde{B}^2A_1-\tilde{X}^2A_1$ , were observed for the metal monopyrrolates. Note that these transitions are labeled by analogy with the CaC<sub>5</sub>H<sub>5</sub> and SrC<sub>5</sub>H<sub>5</sub> molecules, using the orbital symmetries of the C<sub>5v</sub> point group, as will be discussed below. The band origins of the observed vibronic transitions are given in Table I.

Figure 1 shows the  $\tilde{A}^2E_1-\tilde{X}^2A_1$  transition of Ca(C<sub>4</sub>H<sub>4</sub>N). This resolved fluorescence spectrum was recorded by tuning the dye laser probing the molecular transition to the 0-0 band of the  $\tilde{A}^2E_{1(1/2)}-\tilde{X}^2A_1$  spin component. The position of the laser is marked with an asterisk. The strong feature  $76\text{ cm}^{-1}$  to the blue

(8) O'Brien, L. C.; Bernath, P. F. *J. Am. Chem. Soc.* **1986**, *108*, 5017-5018.

(9) Brazier, C. R.; Bernath, P. F.; Kinsey-Nielsen, S.; Ellingboe, L. C. *J. Am. Chem. Soc.* **1986**, *108*, 2126-2132.

(10) Ellingboe, L. C.; Bopeggeda, A. M. R. P.; Brazier, C. R.; Bernath, P. F. *Chem. Phys. Lett.* **1986**, *126*, 285-289.

(11) Brazier, C. R.; Bernath, P. F. *J. Chem. Phys.* **1987**, *86*, 5918-5922; also, *J. Chem. Phys.* **1989**, *91*, 4548-4554.

(12) Bopeggeda, A. M. R. P.; Brazier, C. R.; Bernath, P. F. *Chem. Phys. Lett.* **1987**, *136*, 97-100; *J. Mol. Spectrosc.* **1988**, *129*, 268-275.

(13) Bopeggeda, A. M. R. P.; Brazier, C. R.; Bernath, P. F. *J. Phys. Chem.* **1987**, *91*, 2779-2781.

(14) O'Brien, L. C.; Brazier, C. R.; Bernath, P. F. *J. Mol. Spectrosc.* **1988**, *130*, 33-45.

(15) Brazier, C. R.; Bernath, P. F. *J. Chem. Phys.* **1988**, *88*, 2112-2116.

(16) O'Brien, L. C.; Bernath, P. F. *J. Chem. Phys.* **1988**, *88*, 2117-2120.

(17) West, J. B.; Bradford, R. S.; Eversole, J. D.; Jones, C. R. *Rev. Sci. Instrum.* **1975**, *46*, 164-168.

(18) Herzberg, G. *Electronic Spectra of Polyatomic Molecules*; Van Nostrand Reinhold: New York, 1966.

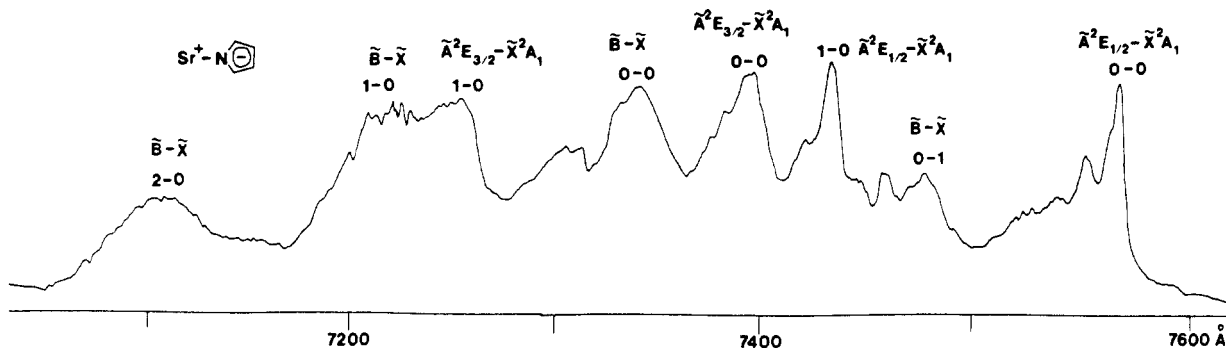


**Figure 3.** The laser excitation spectrum of the strontium monopyrrolate molecule. Two electronic transitions,  $\tilde{A}^2E_1-\tilde{X}^2A_1$  and  $\tilde{B}^2A_1-\tilde{X}^2A_1$ , were observed and assigned. The two spin components of the  $\tilde{A}^2E_1-\tilde{X}^2A_1$  transition are separated by  $300\text{ cm}^{-1}$ . The assignments of the vibronic bands were aided by resolved fluorescence spectra recorded for each vibronic transition.

**TABLE II: Vibrational Frequencies of the Metal-Ligand Stretch of the Calcium and Strontium Monopyrrolate Molecules (in  $\text{cm}^{-1}$ )**

state	Ca( $\text{C}_4\text{H}_4\text{N}$ )	Sr( $\text{C}_4\text{H}_4\text{N}$ )
$\tilde{X}^2A_1$	311	253
$\tilde{A}^2E_{1(1/2)}$	249	237
$\tilde{A}^2E_{1(3/2)}$	241	258
$\tilde{B}^2A_1$		225

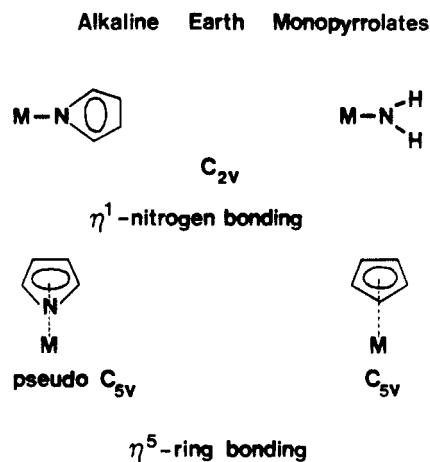
of the laser is the  $\tilde{A}^2E_{1(3/2)}-\tilde{X}^2A_1$  spin component. Emission from the  $\tilde{A}^2E_{1(3/2)}$  spin component occurs because collisions transfer population from the laser-excited  $\tilde{A}^2E_{1(1/2)}$  spin component.

Figure 2 is a resolved fluorescence spectrum of the  $\tilde{B}^2A_1-\tilde{X}^2A_1$  transition of calcium monopyrrolate. The asterisk marks the position of the laser, tuned to the 0-0 band of the  $\tilde{B}-\tilde{X}$  transition. In both Figures 1 and 2, several broad features are seen to the red of the laser. When the laser excites the 0-0 band of a given electronic transition, emission to excited vibrational levels of the ground electronic state occurs. Only the metal-ligand vibrational modes were found to be Franck-Condon active in the electronic spectrum. Therefore, the observed progression, separated by  $\approx 300\text{ cm}^{-1}$ , is assigned to the metal-ligand stretching vibration. These spectra were very useful in obtaining the vibrational frequencies for the ground and excited electronic states, which are reported in Table II.

Figure 3 is a laser excitation spectrum of the strontium monopyrrolate molecule, recorded by scanning the wavelength of the dye laser probing the molecular transition. The assignments provided on this figure were made by using the laser excitation spectrum as well as several resolved fluorescence spectra recorded by individual vibronic transitions. Two electronic transitions,  $\tilde{A}^2E_1-\tilde{X}^2A_1$  and  $\tilde{B}^2A_1-\tilde{X}^2A_1$ , were observed and assigned as shown on the figure. The band origins of these transitions are given in Table I. The two spin components  $\tilde{A}^2E_{1(1/2)}-\tilde{X}^2A_1$  and  $\tilde{A}^2E_{1(3/2)}-\tilde{X}^2A_1$  are separated by  $300\text{ cm}^{-1}$ . Long vibrational progressions in the metal-ligand stretch were observed for the strontium monopyrrolate molecule (see Table I). The metal-ligand stretching frequencies of Sr( $\text{C}_4\text{H}_4\text{N}$ ) molecule were extracted from the low-resolution spectra for the  $\tilde{X}^2A_1$ ,  $\tilde{A}^2E_1$ , and  $\tilde{B}^2A_1$  electronic states. These are reported in Table II. The  $\tilde{A}^2E_{1(3/2)}-\tilde{X}^2A_1$  transition and the  $\tilde{B}^2A_1-\tilde{X}^2A_1$  transition of strontium monopyrrolate are separated by only  $\approx 100\text{ cm}^{-1}$ . As a result, there are several vibronic bands of these two electronic transitions that are close to one another. Therefore, it is not possible to selectively excite one of these bands with a dye laser, without simultaneously exciting others which are close by. This made the assignment of spectra more difficult for the strontium monopyrrolate molecule than for the calcium monopyrrolate molecule.

## Discussion

Figure 4 shows the two possible ways in which the pyrrolate ligand ( $\text{C}_4\text{H}_4\text{N}^-$ ) can bond to the alkaline-earth metal. The bonding can be through the N atom, in which case the metal  $\eta^1$ -monopyrrolates will have  $C_{2v}$  symmetry, or the pyrrolate anion can ring-bond to the metal to produce metal  $\eta^5$ -monopyrrolates



**Figure 4.** Possible ways in which the pyrrolate anion ( $\text{C}_4\text{H}_4\text{N}^-$ ) can bond to the alkaline-earth-metal cation and the subsequent symmetries of the metal monopyrrolate molecule.

of pseudo- $C_{5v}$  symmetry. If the bonding is through the N atom, the resulting metal monopyrrolates should be similar to the metal monoamides ( $\text{MNH}_2$ ) and the metal monoalkylamides ( $\text{MNR}$ , R = alkyl group) which have been studied previously.<sup>13</sup> In this case, three electronic transitions,  $\tilde{A}^2B_2-\tilde{X}^2A_1$ ,  $\tilde{B}^2B_1-\tilde{X}^2A_1$ , and  $\tilde{C}^2A_1-\tilde{X}^2A_1$ , will be observed for the metal monopyrrolates similar to the metal monoamides. If, however, the pyrrolate ligand ring bonds to the metal, the metal monopyrrolates will closely resemble the isoelectronic metal cyclopentadienides,  $\text{M}(\text{C}_5\text{H}_5)$ , which are of  $C_{5v}$  symmetry.<sup>8</sup> A close examination of the spectra indicates that of the metal monopyrrolates are similar to those of the metal cyclopentadienides. Like the cyclopentadienide derivatives, calcium and strontium monopyrrolates seem to have two excited electronic states  $\tilde{A}^2E_1$  and  $\tilde{B}^2A_1$ , with the  $\tilde{A}^2E_1$  state split by spin-orbit interaction into  $\tilde{A}^2E_{1(1/2)}$  and  $\tilde{A}^2E_{1(3/2)}$  spin components. Therefore, it was concluded that the ( $\text{C}_4\text{H}_4\text{N}$ ) ligand ring bonds to the metal and the geometry of the  $\text{M}^+(\text{C}_4\text{H}_4\text{N}^-)$  molecule is pseudo- $C_{5v}$ .

The  $\text{C}_4\text{H}_4\text{N}^-$  ion is a closed-shell ligand. The molecular orbitals of the metal monopyrrolates can be treated as the orbitals of the  $\text{M}^+$  ion perturbed by the  $\text{C}_4\text{H}_4\text{N}^-$  ligand. The Ca<sup>+</sup>/Sr<sup>+</sup> ion contains a single unpaired electron in the  $ns$  ( $n = 4$  for Ca,  $n = 5$  for Sr) valence orbital. In the  $C_{5v}$  point group, the  $ns$  orbital is of  $a_1$  symmetry resulting in a  ${}^2A_1$  ground electronic state for the  $\text{M}(\text{C}_4\text{H}_4\text{N})$  molecules, as shown in Figure 5. Although the  $\text{M}(\text{C}_4\text{H}_4\text{N})$  molecule is of  $C_s$  symmetry, the molecular orbitals are described by using the symmetry symbols of the  $C_{5v}$  point group. There is such a strong correspondence between the spectra of  $\text{M}(\text{C}_4\text{H}_4\text{N})$  and  $\text{M}(\text{C}_5\text{H}_5)$  molecules that this is useful.

The degeneracy of the metal d orbitals is lifted in the  $C_{5v}$  point group to produce orbitals with symmetries  $e_2(d_{x^2-y^2}, d_{xy})$ ,  $e_1(d_{xz}, d_{yz})$ , and  $a_1(d_{z^2})$ . The degenerate p orbitals of the metal provide  $e_1(p_x, p_y)$  and  $a_1(p_z)$  molecular orbitals. The presence of the ligand also mixes the metal p and d orbitals so these molecular orbitals

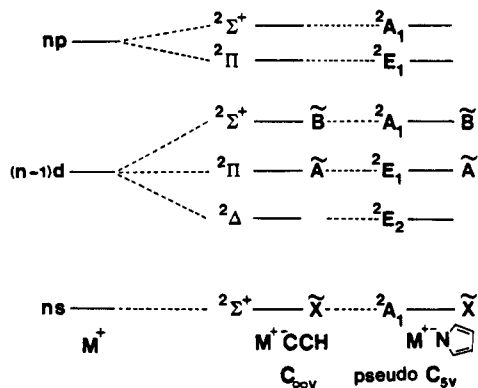


**Figure 5.** Correlation diagram for the orbitals of the  $M^+$  ion perturbed by the  $(C_4H_4N)^-$  ligand. Although the  $(C_4H_4N)^-$  ligand is of  $C_s$  symmetry, the notation given here is from the  $C_{5v}$  point group (see text).

are p-d mixtures. The above molecular orbitals give rise to the  ${}^2E_2$ ,  ${}^2E_1$ ,  ${}^2A_1$ ,  ${}^2E_1$ , and  ${}^2A_1$  electronic states (in the order of increasing energy) for the  $M(C_4H_4N)$  molecule as illustrated in Figure 5.

Electronic transitions from the  $\tilde{X}^2A_1$  ground state to the  ${}^2E_2$  state are forbidden by the electric dipole selection rules. Note that the lower symmetry ( $C_s$ ) of the  $M(C_4H_4N)$  molecule could make the  ${}^2E_2 \rightarrow {}^2A_1$  transition allowed but no evidence of this transition was found. Therefore, the first observed electronic transition of  $M(C_4H_4N)$  molecules is assigned as the  $\tilde{A}^2E_1 \rightarrow \tilde{X}^2A_1$  transition. The spin angular momentum and the unquenched orbital angular momentum in the  $\tilde{A}^2E_1$  state couple together to produce the two spin-orbit components  $\tilde{A}^2E_{1(1/2)}$  and  $\tilde{A}^2E_{1(3/2)}$ . These two spin components are separated by the spin-orbit coupling constant  $A$ . For the calcium monopyrrolate molecule  $A$  is  $76 \text{ cm}^{-1}$ , whereas for the strontium analogue it is  $300 \text{ cm}^{-1}$ . This is slightly higher than the values reported for metal monocyclopentadienides ( $A = 57 \text{ cm}^{-1}$  for  $Ca(C_5H_5)$  and  $255 \text{ cm}^{-1}$  for  $Sr(C_5H_5)^2$ ) and the metal monohydroxides ( $A = 67 \text{ cm}^{-1}$  for  $CaOH$  and  $264 \text{ cm}^{-1}$  for  $SrOH$ <sup>19,20</sup>) but not unreasonable for the  $Ca^+$  ( $Sr^+$ ) ion perturbed by ligands of  $C_{\infty v}$ ,  $C_{3v}$ , or  $C_{5v}$  symmetry. These observations are closely related to the often successful semiempirical estimation of diatomic spin-orbit coupling constants from the corresponding atomic values (for example, ref 23). The  $\tilde{A}$  state spin-orbit splittings of several alkaline earth metal containing free radicals are reported in Table III for comparison purposes. The observation of spin-orbit splitting in the  $\tilde{A}^2E_1$  state of the metal monopyrrolates confirmed that these free radicals effectively have high symmetry, most probably pseudo- $C_{5v}$ .

(19) Brazier, C. R.; Bernath, P. F. *J. Mol. Spectrosc.* **1985**, *114*, 163-173.

(20) Bernath, P. F.; Brazier, C. R. *Astrophys. J.* **1985**, *288*, 373-376.

(21) Bernath, P. F.; Field, R. W. *J. Mol. Spectrosc.* **1980**, *82*, 339-347.

(22) Steimle, T. C.; Domaille, P. J.; Harris, D. O. *J. Mol. Spectrosc.* **1978**, *73*, 441-443.

(23) Lefebvre-Brion H.; Field, R. W. *Perturbations in the Spectra of Diatomic Molecules*; Academic Press: Orlando, FL, 1986; p 216.

**TABLE III: Observed Spin-Orbit Splittings for the  $\tilde{A}^2\Pi$  or  $\tilde{A}^2E$  States of Some Alkaline Earth Metal Containing Free Radicals, ML (in  $\text{cm}^{-1}$ ), Where  $M = Ca$  or  $Sr$  and  $L$  Is a Ligand**

molecule	CaL	SrL
$MF^a$	73	281
$MOH^b$	67	264
$MOCH_3^c$	65	268
$MCCH^d$	70	275
$MN_3^e$	76	296
$MNCO^f$	68	293
$MCH_3^g$	73	309
$MC_5H_5^h$	57	255
$MC_4H_4N^i$	76	300

<sup>a</sup>References 21 and 22. <sup>b</sup>References 19 and 20. <sup>c</sup>References 9 and 14. <sup>d</sup>Reference 12. <sup>e</sup>Reference 15. <sup>f</sup>References 10 and 16. <sup>g</sup>Reference 11. <sup>h</sup>Reference 8. <sup>i</sup>This work.

The higher energy electronic transition observed is assigned as the  $\tilde{B}^2A_1 \rightarrow \tilde{X}^2A_1$  transition. For the metal monopyrrolate molecules, the  $\tilde{A}$  and  $\tilde{B}$  electronic states are relatively close in energy (see Table I) compared to the  $\tilde{A}$  and  $\tilde{B}$  states in the metal cyclopentadienides.<sup>8</sup> This tends to complicate the spectra of the metal monopyrrolates, particularly those of the strontium monopyrrolate molecule where the  $\tilde{B}^2A_1$  state and the  $\tilde{A}^2E_{1(3/2)}$  spin component are separated by only  $\approx 100 \text{ cm}^{-1}$ . A similar problem was encountered when assigning the spectra of strontium monocyclopentadienide for which the spin-orbit coupling constant matched the metal-ligand stretching vibrational frequency.<sup>8</sup> The assignments provided here were made by comparison of the spectra of the  $Sr(C_4H_4N)$  and  $SrC_5H_5$  molecules.

The electronic transitions of the metal monopyrrolate molecules occur on metal-centered orbitals so the Franck-Condon factors favor those vibrations that are associated with the metal atom. Therefore, the vibronic bands reported are all assigned to a single metal-ligand stretching vibration. Progressions in this vibrational mode were observed for both molecules in all of the electronic transitions reported here. The observation of a progression in the metal-ligand mode suggests that the metal-ligand bond distances (cf. vibrational frequencies, Table II) are different in the various electronic states. The reported frequencies have an estimated uncertainty of  $\pm 10 \text{ cm}^{-1}$ .

## Conclusion

In our continuing study of the gas-phase inorganic chemistry of Ca and Sr, we have discovered the  $Ca(C_4H_4N)$  and  $Sr(C_4H_4N)$  molecules. These monopyrrolate free radicals were found to be ring-bonding ( $\eta^5$ ) like the isoelectronic monocyclopentadienyl molecules, rather than nitrogen-bonding ( $\eta^1$ ) like the monoalkylamide derivatives. Our assignments of the spectra rest largely on the comparison between the electronic spectra of  $Ca(C_4H_4N)$  and  $Sr(C_4H_4N)$  with the isoelectronic  $CaC_5H_5$  and  $SrC_5H_5$  molecules.

**Acknowledgment.** This research was supported by the National Science Foundation (CHE-8608630).